Effects of Hydration during Drilling on Fracability of Shale Oil Formations: A Case Study of Da’anzhai Section Reservoir in Sichuan Basin, China

Authors:

Guangfu Zhang, Haibo Wang, Fengxia Li, Di Wang, Ning Li, Shiming He

Date Submitted: 2023-02-21

Keywords: shale oil reservoir, brittleness index, fracability index, hydration, Da’anzhai shale, fracture initiation pressure

Abstract:

Accurate evaluation of shale oil reservoir fracability helps avoid blind fracturing and ensures efficient fracturing. However, the current evaluation of the fracability index rarely considers the impact of hydration caused by drilling fluid invasion during drilling. The results of a rock triaxial mechanical test conducted to evaluate the mechanical properties of shale oil reservoirs are reported in this paper. Based on the results, we developed a comprehensive evaluation method of shale oil reservoir fracability that considers hydration; the effects of the brittleness index, horizontal difference stress, and fracture toughness; and the law of water phase intrusion into shale oil reservoirs. The research results show that the average compressive strength decreased by 37.99%, the average elastic modulus decreased by 53.36%, and the average Poisson’s ratio increased by 68.75% after being soaked for 48.00 h at 80 °C and 30.00 MPa. The water saturation rate at the borehole wall was the highest; with the extension to the stratum, it gradually decreases to the original water saturation rate of the formation, while the fluctuation radius gradually increases with time. The Young’s modulus and fracture toughness decrease, the Poisson’s ratio increases, and the fracability index reaches a maximum value at the wellbore (i.e., the highest water saturation rate), indicating that the strength of the hydrated rock decreases and it can be easily fractured. The case analysis shows that the optimal fracturing position of the Da’anzhai Section of Well NC2H is around 2600 m deep. After the hydration occurs, the fracture initiation pressure of the formation is reduced from the original value of 72.31 MPa to 66.80 MPa. This indicates that when hydration decreases, the formation fracture pressure also increases. The research presented in this paper can be used to optimize fracture location and set a reasonable fracturing pressure.

Record Type: Published Article

Submitted To: LAPSE (Living Archive for Process Systems Engineering)

Citation (overall record, always the latest version):	LAPSE:2023.0842
Citation (this specific file, latest version):	LAPSE:2023.0842-1
Citation (this specific file, this version):	LAPSE:2023.0842-1v1

DOI of Published Version: https://doi.org/10.3390/pr10112313

processes

MDPI

Article

Effects of Hydration during Drilling on Fracability of Shale Oil Formations: A Case Study of Da'anzhai Section Reservoir in Sichuan Basin, China

Guangfu Zhang [1,2,3], Haibo Wang [1,2], Fengxia Li [1,2], Di Wang [1,2], Ning Li [1,2] and Shiming He [1,2,3,*]

[1] State Key Laboratory of Shale Oil and Gas Enrichment Mechanisms and Effective Development, Research Institute of Petroleum Exploration and Development of SINOPEC, Beijing 100038, China
[2] State Energy Center for Shale Oil Research and Development, Beijing 100728, China
[3] State Key Laboratory of Oil and Gas Reservoir Geology and Exploitation, Southwest Petroleum University, Chengdu 610500, China
* Correspondence: hesm-swpu@sohu.com

Highlights:

1. How to quantitative evaluation of mechanical properties of shale in Da'anzhai section combined with triaxial mechanical experiments?

- The compressive strength of dry rock samples and soaked rock samples were tested by triaxial mechanical experiments.
- According to the stress-strain curves, the changes of compressive strength, elastic modulus and Poisson's ratio before and after hydration were analyzed.

2. How to establish a mathematical model of shale fracability that comprehensively considers brittleness index, horizontal differential stress, and fracture toughness is proposed?

- Fracability index is proportional to brittleness index and horizontal differential stress, and inversely proportional to fracture toughness.
- Young 's modulus, Poisson's ratio and tensile strength in fracability index model are related to rock water saturation, so the fracturing index is also related to rock hydration.

3. What is the effect of shale hydration on fracability and fracture pressure?

- As the water saturation rate of the rock gradually decreases, the FI of the formation rock de-creases
- Combined with the variation law of water saturation rate, it shows that after the shale around the well is hydrated, the fracture pressure of the formation decreases

Abstract: Accurate evaluation of shale oil reservoir fracability helps avoid blind fracturing and ensures efficient fracturing. However, the current evaluation of the fracability index rarely considers the impact of hydration caused by drilling fluid invasion during drilling. The results of a rock triaxial mechanical test conducted to evaluate the mechanical properties of shale oil reservoirs are reported in this paper. Based on the results, we developed a comprehensive evaluation method of shale oil reservoir fracability that considers hydration; the effects of the brittleness index, horizontal difference stress, and fracture toughness; and the law of water phase intrusion into shale oil reservoirs. The research results show that the average compressive strength decreased by 37.99%, the average elastic modulus decreased by 53.36%, and the average Poisson's ratio increased by 68.75% after being soaked for 48.00 h at 80 °C and 30.00 MPa. The water saturation rate at the borehole wall was the highest; with the extension to the stratum, it gradually decreases to the original water saturation rate of the formation, while the fluctuation radius gradually increases with time. The Young's modulus and fracture toughness decrease, the Poisson's ratio increases, and the fracability index reaches a maximum value at the wellbore (i.e., the highest water saturation rate), indicating that the strength of the hydrated rock decreases and it can be easily fractured. The case analysis shows that the optimal fracturing position of the Da'anzhai Section of Well NC2H is around 2600 m deep. After the

check for updates

Citation: Zhang, G.; Wang, H.; Li, F.; Wang, D.; Li, N.; He, S. Effects of Hydration during Drilling on Fracability of Shale Oil Formations: A Case Study of Da'anzhai Section Reservoir in Sichuan Basin, China. *Processes* **2022**, *10*, 2313. https://doi.org/10.3390/pr10112313

Academic Editors: Jan Vinogradov, Ali Habibi and Zhengyuan Luo

Received: 2 August 2022
Accepted: 26 October 2022
Published: 7 November 2022

Publisher's Note: MDPI stays neutral with regard to jurisdictional claims in published maps and institutional affiliations.

hydration occurs, the fracture initiation pressure of the formation is reduced from the original value of 72.31 MPa to 66.80 MPa. This indicates that when hydration decreases, the formation fracture pressure also increases. The research presented in this paper can be used to optimize fracture location and set a reasonable fracturing pressure.

Keywords: shale oil reservoir; brittleness index; fracability index; hydration; Da'anzhai shale; fracture initiation pressure

1. Introduction

In 2018, Sinopec estimated that the technically recoverable resources of shale oil in China were (74–372)10^8 t. The continental shale oil and gas resources in the Sichuan Basin accounted for 30% of the national shale oil and gas geological reserves and 40% of the technically recoverable reserves. Shale oil reservoirs generally do not have natural productivity, while their fracability depends on the degree of natural fracture development, the mineral composition of the rock [1] (Fathy 2021), and the mechanical properties of the rock [2,3] (Du 2019; Zou 2019).

Studies have shown that the reservoir space type of the shale reservoirs in the Da'anzhai Section of the Ziliujing Formation in the Yuanba and Fuling areas is primarily inorganic pores, and the shale porosity ranges from 1.5% to 6.7%, with an average of 3.9% [4] (Zhou 2020). Affected by the drilling pressure difference and chemical potential, the drilling fluid intrudes into the rock along the pores and bedding fractures, reducing the strength of the rock body and weak plane. The concentration of clay minerals in the shale is relatively high; illite, montmorillonite, and montmorillonite-mixed layers have strong hydration ability. Under the influence of hydration stress, ion transport, film effect, and solute diffusion, clay minerals are easily hydrated, thus reducing the rock strength [5–7] (Muniz 2005; van Oort E 1996; Wang 2006). Many studies have attempted to describe this phenomenon: Yew and Chenevert [8] (1990) proposed a model for calculating the amount of adsorbed water after quantitatively analyzing the mechanochemical coupling. Hale and Mody [9] (1993) pointed out that the chemical kinetic factors that cause rock deformation and failure mainly include [10] (2011) van der Waals force, electrostatic attraction, plate potential energy, capillary tension, matrix suction, osmotic pressure, and concentration polarization boundary resistance. He [11] (2020) explored the deformation and failure law of rational shale under the action of mechanical–chemical coupling. Therefore, the shale mechanical–chemical coupling methods can be divided into the following: water transport mechanism in shale, equivalent pore pressure method, total adsorbed water correlation method, and incremental elasticity theory of total water potential [12] (Deng 2003).

To study shale fracability, scholars have established different evaluation methods based on different physical parameters and mathematical theories. Many scholars [13–18] (Rickman 2008; Tang 2012; Enderlin 2011; Mullen 2012; Yuan 2013; Zhang 2014) deem that the normalized average value of Young's modulus and Poisson's ratio are used as a brittleness index to characterize rock fracability. Zhang [19,20] (2013; 2019) believed that the brittleness index and the plasticity coefficient should both be used to evaluate the shale fracability. To this end, they carried out numerous experiments and proposed a rock-brittleness evaluation method based on triaxial compression energy dissipation. Mike J. Mullen [21] (2012) deemed that the fracability should consider reservoir sedimentary characteristics and mineral content composition. Chen [22] (2001) evaluated the fracability of shale reservoirs in terms of rock mechanics. Yuan [17] (2013) established a fracability evaluation model using three parameters: the elastic modulus, Poisson's ratio, and uniaxial tensile strength. Zhao [23] (2015) used shale brittleness and fracture toughness to evaluate shale fracability. Sui [24] (2016) discussed how fracability is affected by the clay mineral content, cohesion, and internal friction angle. Yue [25] (2019) established a fuzzy comprehensive evaluation model of fracability based on the fuzzy mathematics theory and the

analytic-hierarchy-process–entropy method. Ma [26] (2019) focused on the lacustrine shale reservoirs located in the Dongying Sag and the Subei Basin. The results showed that the macrostructure, mineral content, lithology, and the presence of microfractures in the shale are the main factors affecting its brittleness. Considering the fracture toughness of carbonate minerals and the plastic effect of organic matter, a formula for calculating the brittleness index based on the mineral composition method was proposed. Jia [27] (2020) explored the mineralogical composition, microstructure formation, static elastic properties, fracture toughness, and mechanical anisotropy of the Longmaxi shale through a series of laboratory geomechanical and petrophysical experiments. Four factors, namely brittleness, quartz content, diagenesis, and natural fracture, were analyzed to determine the fracability of the shale in the Lower Cambrian Niutitang Formation, Northwestern Hunan [28] (Wu 2018). Brittle rocks can have higher fracture toughness, making their fracture more difficult. Iyare [29] (2022) used an existing fracability evaluation model describing the brittleness, fracture toughness, and minimum horizontal in situ stress to evaluate the fracability of the four lithofacies within the Naparima Hill Formation. Brittleness indices based on the rock elastic properties, rock strength, and mineral concentrations were used to evaluate the rock brittleness, while the fracture toughness was determined from the tensile strength.

However, the previous fracability evaluation methods considered a single factor or a simple superposition of multiple factors, failing to capture the physical and chemical reactions between the working fluid and shale. Studies have shown that shale contains a larger number of clay minerals and has a strong hydration ability. After hydration, the rock strength of shale will be greatly reduced, and creep will occur simultaneously, changing the crack structure. Therefore, the chemical interaction between the working fluid and the shale cannot be ignored. By considering the influence of hydration, the fracturability of shale oil reservoirs can be characterized more comprehensively.

The research in this paper mainly focuses on the following three parts: (1) Through experiments, the changes in the rock mechanical properties of the shale oil reservoirs before and after soaking are analyzed, and the changing laws of rock mechanical parameters are recorded. (2) We analyze the law of water-based drilling fluid invading shale oil reservoirs under the action of chemical potential. (3) Considering the rock-brittleness index, horizontal difference stress, and fracture toughness, a set of fracability evaluation methods suitable for shale oil reservoirs is formed. (4) Taking Well NC2H as an example, we predicted the fracability index of the Da'anzhai Section at different depths, selected the most suitable sweet spot position for fracturing, and calculated the corresponding fracturing pressure.

2. Shale Mechanics Experiment

Young's modulus and Poisson's ratio are the principal rock mechanical parameters that are used to characterize shale brittleness [13] (RICKMAN 2008). The Young's modulus reflects the ability of shale to maintain fractures after being fractured, while the Poisson's ratio reflects the ability of shale to fracture under pressure. The higher the Young's modulus of shale and the lower the Poisson's ratio, the stronger the brittleness is. By comparing the changes in the mechanical parameters of the shale before and after soaking, we shed further insight into the effect of hydration on rock fracability.

2.1. Sample Preparation

In this experiment, eight standard rock samples were prepared and used to test the mechanical properties of the shale before and after soaking, labeled A, B, C, D, E, F, G, and H, and the size of the rock samples was Φ 25 mm $\times$ 50 mm, where A, B, C, and D are dry rock samples, and four rock samples, E, F, G, and H, are soaked. The soaking conditions are as follows: pressure of 30 MPa, time of 48 h, and temperature of 80 °C.

2.2. Methodology

To study the mechanical parameters of the Da'anzhai shale formation in Central Sichuan in the downhole stress environment, the triaxial mechanical test was carried out.

The GCTS triaxial mechanical testing machine was used to test and analyze the triaxial compressive strength, elastic modulus, and Poisson's ratio of the Da'anzhai formation shale in the downhole stress environment. Experimental scheme: First, a triaxial mechanical test was performed on four groups of dry rock samples (A, B, C, and D); the experimental confining pressure was set to 30 MPa, and the triaxial compressive strength, elastic modulus, and Poisson's ratio of the dry rock samples were calculated according to the stress–strain curve. Similarly, triaxial mechanical tests were performed on four groups of soaked rock samples (E, F, G, and H), and the experimental confining pressure was set to 30 MPa. According to the stress–strain curve, the triaxial compressive strength, elastic modulus, and Poisson's ratio of the soaked shale were calculated. Finally, the experimental data were counted, and the test results were compared and analyzed.

2.3. Test Results and Analysis

The results of the triaxial mechanical experiments are shown in Figure 1.

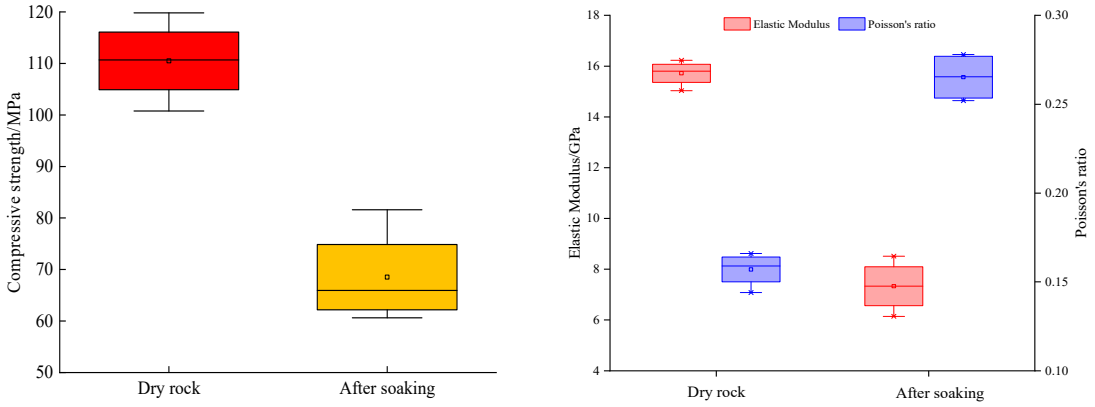

Figure 1. Changes in rock mechanical parameters before and after soaking (compressive strength on the **left**, and elastic modulus and Poisson's ratio on the **right**).

When comparing the dry rock sample and the soaked rock sample, we found that, under the same confining pressure, the average compressive strength of the dry rock sample was 110.50 MPa, the average elastic modulus was 15.719 GPa, and the average Poisson's ratio was 0.16. The average compressive strength of the soaked rock samples was 68.52 MPa, a decrease of 37.99%; the average elastic modulus was 7.332 GPa, a decrease of 53.36%; and the average Poisson's ratio was 0.27, an increase of 68.75%. After soaking, the compressive strength and elastic modulus of the shale decreased sharply, while the Poisson's ratio increased, indicating that the mechanical strength and elastic parameters of the shale rock in the Da'anzhai Section were obviously affected by the drilling fluid soaking. This also showed that the water saturation rate of the shale also changed, causing changes in formation fracability.

The triaxial test curves of rock samples A, B, G, and H are shown in Figure 2. E_v is the vertical strain, E_a is the volumetric strain, and E_r is the radial strain. The figure shows that the compressive strength of the shale after soaking is significantly reduced, the rock brittleness is reduced, the plasticity is enhanced, and the residual strength can still be maintained after failure.

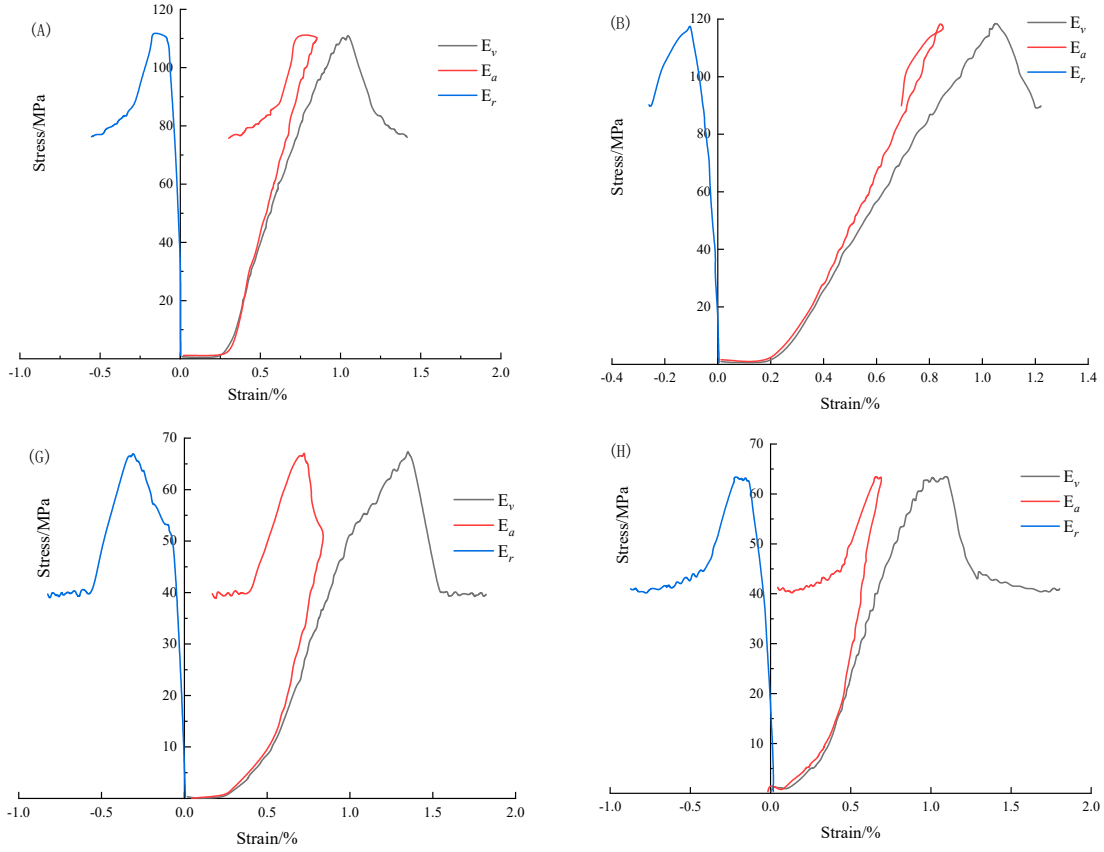

Figure 2. Triaxial mechanical experiment test curve.

3. Fracability Evaluation Method Considering Hydration

First, the three indexes, namely brittleness index, in situ stress, and fracture toughness, were selected to establish a fracability evaluation model. Then the mathematical model of water phase intrusion into shale oil reservoir was deduced, and both the law of influence of hydration on the brittleness index (Young's modulus and Poisson's ratio) and fracture toughness were obtained. Finally, the effect of hydration on the fracability index was calculated.

3.1. Fracability Index Model

Fracability reflects the shale geology and reservoir characteristics, while it is affected by many factors. According to the research experience of scholars on the fracability of shale gas reservoirs, the brittleness index represents the difficulty of shale fracturing. At present, the commonly used calculation methods of the brittleness index include the Young's modulus and Poisson's ratio [13] (RICKMAN 2008). This method makes it easy to obtain data, and it is more closely integrated with the field and more widely used. In this paper, the elastic modulus of rock refers to the Young's modulus for calculation:

$$\begin{cases} YM_{BRIT} = \frac{YM - YM_{cmin}}{YM_{cmax} - YM_{cmin}} \times 100\% \\ PR_{BRIT} = \frac{PR - PR_{cmin}}{PR_{cmax} - PR_{cmin}} \times 100\% \\ B_{rit} = \frac{YM_{BRIT} + PR_{BRIT}}{2} \end{cases} \quad (1)$$

where B_{rit} is the brittleness index, 0–1; YM is the static Young's modulus; YM_{cmax} and YM_{cmin} are the maximum and minimum static Young's modulus, respectively, GPa; YM_{BRIT} is the normalized Young's modulus, 0–1; PR is the static Poisson's ratio; PRcmax and PRcmin are, respectively, the largest and smallest static Poisson's ratio in the region, dimensionless; and PR_{BRIT} is the normalized Poisson's ratio, 0–1.

The research results show that, in addition to overcoming the tensile strength of the rock body, the net pressure in the fracture also must overcome the horizontal stress difference. This should enable the fracture to open and extend, forming a complex fracture network [30,31] (Chen 2020; Lian 2022). The horizontal difference stress coefficient, K_h, is expressed as follows:

$$K_h = \frac{\sigma_H - \sigma_h}{\sigma_h} \tag{2}$$

where K_h is the horizontal difference stress coefficient, dimensionless; σ_H is the maximum horizontal in situ stress, MPa; and σ_h is the horizontal minimum ground stress, MPa.

Fully determining the fracability of the reservoir does not rely only on the elastic modulus and Poisson's ratio. For example, the elastic modulus and Poisson's ratio of some rocks are similar, but the brittleness greatly differs. The important difference is the fracture toughness. Fracture toughness is crucial for characterizing the difficulty of reservoir fracturing, which reflects the ability to maintain the forward extension of the fracture after its formation.

The type I fracture toughness (K_{Ic}) and type II fracture toughness (K_{IIC}) of shale can be calculated from the confining pressure and uniaxial tensile strength (S_t) on the fracture surface [22,32,33] (Chen 1997; Jin 2001,2011). The calculation methods are as shown in Formulas (3) and (4):

$$K_{IC} = 0.2176\sigma_n + 0.0059S_t^3 + 0.0923S_t^2 + 0.517S_t - 0.3322 \tag{3}$$

where σ_n is the confining pressure on the crack surface, MPa; S_t is the uniaxial tensile strength, MPa; and K_{Ic} is the fracture toughness, MPa·m$^{0.5}$.

$$K_{IIC} = 0.0956\sigma_n + 0.1383S_t - 0.0820 \tag{4}$$

The rock mechanical parameters involved in the calculation method of types I and II fracture toughness, such as uniaxial tensile strength and confining pressure, can be obtained from logging data. The calculation method is as follows:

$$\begin{cases} \sigma_c = (0.0045 + 0.0035V_{cl})E_d \\ S_t = \sigma_c / K \end{cases} \tag{5}$$

where V_{cl} is the clay volume, dimensionless; E_d is the dynamic elastic modulus, GPa; and K is a constant, K = 12.26:

$$\begin{cases} K_{ICn} = \frac{K_{ICmax} - K_{IC}}{K_{ICmax} - K_{ICmin}} \\ K_{IICn} = \frac{K_{IImax} - K_{IIC}}{K_{IImax} - K_{IImin}} \\ K_n = \frac{K_{ICn} + K_{IICn}}{2} \end{cases} \tag{6}$$

To determine the confining pressure, the confining pressure acting on the fracture surface of the n-th branch fracture of shale gas fracturing can be expressed as [34] follows:

$$\sigma_n = n \begin{bmatrix} \sigma_h & & \\ & \sigma_H & \\ & & \sigma_v \end{bmatrix} n^T \tag{7}$$

where n = [cos βsin θ, sin βcos θ, sin β]; β is the fracture dip angle; θ is the angle between the fracture strike and the well axis; and σ_v is the overburden pressure, MPa;

According to the above studies, the fracability of shale gas reservoirs is obviously positively correlated with the brittleness index and negatively correlated with the fracture toughness. Considering the brittleness index, in situ stress, and rock fracture toughness, a new model for fracability evaluation is established in this paper, as shown in Equation (8).

$$FI = \frac{a * B_{rit} + b * K_h}{K_n} \tag{8}$$

where *FI* is the fracability index; a and b are constant coefficients, dimensionless.

According to the classical rock mechanics theory, the fracture of the rock during hydraulic fracturing is caused by the excessive density of the fracturing fluid in the well, which causes the stress on the rock to exceed the tensile strength. The fracture initiation pressure when the rock produces tensile failure is as follows [35] (Jin 2012):

$$p_f = \frac{3\sigma_h - \sigma_H - \delta\left[\frac{\alpha_1(1-2\nu)}{1-\nu} - \phi\right]p_p + S_t - \alpha_1 p_p}{1 - \delta\left[\frac{\alpha_1(1-2\nu)}{1-\nu} - \phi\right]} \tag{9}$$

When the formation permeability is low, δ equals 0, as shown with the following equation:

$$p_f = 3\sigma_h - \sigma_H - \alpha_1 p_p + S_t \tag{10}$$

3.2. Analysis of the Law of Water Phase Intrusion into Shale Oil Reservoirs

During the drilling of shale oil reservoirs, the pressure difference and capillary force will jointly affect the entry of the water-based drilling fluid into the oil layer and change the water saturation rate of the formation rocks around the well. Therefore, for different shale oil reservoirs, different curve characteristics and different J_0 functions will be obtained according to the experiment [36] (Buckley 1942). The expression of the J_0 function is as follows:

$$J_0(S) = \frac{1}{\sigma_{\mathrm{ow}} \cos\theta_{\mathrm{ow}}} p_c(S)\sqrt{\frac{K_f}{\phi}} \tag{11}$$

where σ_{ow} is the surface tension of the oil–water interface, N m; θ is the contact angle of the oil–water interface, °; $p_{\mathrm{c}}(S)$ is the function of the capillary force with saturation; and φ is the shale oil reservoir porosity, %.

According to the J_0 function, the expression of the capillary force function can be derived as follows [37] (Jiang 2014):

$$p_c(S_w) = \frac{J(S_w)\sigma_{\mathrm{ow}} \cos\theta_{\mathrm{ow}}}{\left(\frac{K_f}{\phi}\right)^{0.5}} = 0.1767e^{-0.05572S_w}\frac{\sigma_{\mathrm{ow}} \cos\theta_{\mathrm{ow}}}{\left(\frac{K_f}{\phi}\right)^{0.5}} \tag{12}$$

According to Formula (12), the capillary force is related to formation wettability. When the size of the wetting contact angle changes, the positive and negative capillary force can be directly changed; that is, the wetting reversal occurs. When a water-based fluid is used to drill a shale oil reservoir, the fluid flow near the wellbore is an oil–water two-phase flow process. Therefore, the model assumes the following conditions:

1. Shale oil reservoirs are hydrophilic and isotropic;
2. During drilling fluid intrusion into shale oil layer, the fluid viscosity and volume coefficient remain unchanged;
3. During the whole two-phase flow process, the gravity effect is not considered, and the oil and water are immiscible when in contact with each other.

Based on the above model assumptions, according to Darcy's law of oil–water two-phase flows, we obtain the following:

$$\begin{cases} v_w = \frac{K_f K_{\mathrm{rw}}}{\mu_w}\frac{\partial p_w}{\partial r} \\ v_o = \frac{K_f K_{\mathrm{ro}}}{\mu_o}\frac{\partial p_o}{\partial r} \end{cases} \tag{13}$$

where K_{rw} is the relative permeability of the water phase of shale oil reservoir; v_{w} is the water phase velocity, m/s; μ_{w} is the water phase viscosity, mPa·s; p_{w} is the water phase pressure, Pa; K_{ro} is Oil phase relative permeability, dimensionless; v_{o} is the oil phase velocity, m/s; μ_{o} is the oil phase viscosity, mPa·s; and p_{o} is oil phase pressure, Pa.

In the process of drilling fluid intrusion into the reservoir, the oil–water two-phase continuity equation is as follows:

$$\begin{cases} \nabla\left[\frac{K_w(S_w)}{\mu_w}\nabla p_w\right] = \phi\frac{\partial S_w}{\partial t} \\ \nabla\left[\frac{K_o(S_w)}{\mu_o}\nabla p_o\right] = \phi\frac{\partial S_o}{\partial t} \end{cases} \tag{14}$$

where $\bigtriangledown$ is the Laplace operator; K_{w} describes the water permeability of the shale oil reservoir, mD; S_{w} is the water saturation rate, %; K_{o} describes the oil permeability of the shale oil reservoir, mD; S_{o} is the oil saturation, %; and t is the oil–water two-phase seepage time, s.

If the oil phase and water phase volume fracability factors are considered, the drilling fluid invasion model of the oil layer can be obtained:

$$\begin{cases} \frac{1}{r}\frac{\partial}{\partial r}\left(r\frac{KK_{\mathrm{rw}}}{\mu_w B_w}\frac{\partial p_w}{\partial r}\right) = \frac{\partial}{\partial t}\left(\frac{\phi S_w}{B_w}\right) \\ \frac{1}{r}\frac{\partial}{\partial r}\left(r\frac{KK_{\mathrm{ro}}}{\mu_o B_o}\frac{\partial p_o}{\partial r}\right) = \frac{\partial}{\partial t}\left[\frac{\phi S_o}{B_o}\right] \end{cases} \tag{15}$$

In the above model, to combine water phase pressure and oil phase pressure, the water saturation rate and oil saturation, and the absolute permeability and relative permeability of the two phases, the following three auxiliary equations are required [38] (Naseri 2012):

$$p_c(S_w) = p_w - p_o \tag{16}$$

$$S_w + S_o = 1 \tag{17}$$

$$\begin{cases} K_{rw} = A * \left(\frac{S_w - S_{wi}}{1 - S_{wi} - S_{or}}\right)^c \\ K_{ro} = B * \left(1 - \frac{S_w - S_{wi}}{1 - S_{wi} - S_{or}}\right)^c \end{cases} \tag{18}$$

where A, B, and C are all constants which can be obtained from experiments according to the reservoir characteristics. In this paper, the empirical values of a certain oilfield are taken: A = 0.9, B = 0.8, and C = 4; S_{or} and S_{wi} are the residual oil saturation and original water saturation rate of the reservoir, respectively, dimensionless.

According to Equations (16)–(18), there are a total of six dependent variables, namely S_{w}, S_{o}, p_{w}, p_{o}, v_{w}, and v_{o}. The capillary force $p_{\mathrm{c}}(S_{\mathrm{w}})$ can be obtained according to the J_0 function. This set of equations can be solved if the initial and boundary conditions are given.

Initial time: $t = 0, r_w < r < r_e, S_w = S_{wi}$;

Inner boundary conditions of shale oil reservoirs: $\begin{cases} t \geq 0, r = r_w, S_w = 1 - S_{or} \\ t \geq 0, r = r_w, p_o = p_b \end{cases}$;

External boundary conditions of shale oil reservoirs: $\begin{cases} t \geq 0, r = r_e, S_w = 1 - S_{\mathrm{or}} \\ t \geq 0, r = r_e, p_o = p_e \end{cases}$.

where ρ_b is drilling fluid pressure in wellbore, MPa; ρ_e is original oil reservoir pressure, MPa.

The above equations are strongly nonlinear and cannot be analyzed by using conventional analytical methods. Therefore, in this paper, the staggered grid is used to conduct double implicit difference on the above equations. The following differential equation of water-based drilling fluid intrusion into the shale oil reservoir model is obtained:

$$\begin{cases} (rK_{\mathrm{rw}})^j_{i+\frac{1}{2}}\frac{\partial^2 p_w}{\partial r^2} + \frac{\partial(rK_{\mathrm{rw}})}{\partial r}\frac{\partial p_w}{\partial r} = \frac{r_i\phi\mu_w}{K\Delta t}\pi\left({S_w}_i^{j+1} - {S_w}_i^{j}\right) \\ (rK_{\mathrm{ro}})^j_{i+\frac{1}{2}}\frac{\partial^2 p_o}{\partial r^2} + \frac{\partial(rK_{\mathrm{ro}})}{\partial r}\frac{\partial p_o}{\partial r} = \frac{r_i\phi\mu_o}{K\Delta t}\pi\left({S_o}_i^{j+1} - {S_o}_i^{j}\right) \end{cases} \tag{19}$$

According to the mass conservation theory, the formula of water content in the shale oil layer is theoretically derived:

$$W(r,t) = \frac{\rho_{wf} V_w}{\rho_s V_s} = \frac{\rho_{wf} \phi S_w}{\rho_s (1-\phi)} \tag{20}$$

where ρ_{wf} and ρ_s are, respectively, the density of the drilling fluid and shale framework, g/cm^3; V_W and V_S are, respectively, the volume of water in the rock and the volume of the shale framework, cm^3.

Scholars have conducted much experimental research on water absorption [39] (Huang 1995) and concluded that the elastic modulus and Poisson's ratio change regularly with the water saturation rate of shale:

$$\frac{dE}{dW} = -\frac{E_1 E_2}{2(W-W_a)^{\frac{1}{2}}} exp\left[-E_2 (W-W_a)^{\frac{1}{2}}\right] \tag{21}$$

$$\frac{d\nu}{dW} = 1.3 \tag{22}$$

where E is the elastic modulus of rock after water absorption, MPa; E_1 and E_2 are coefficients, which can be obtained from experiments; the empirical values are 4×10^4 and -11; W and W_a are the mass percentage of adsorbed water and the mass percentage of original water content, %; and ν is the Poisson's ratio of rock formation after water absorption.

According to Equations (20) and (21) and data listed in Table 1, from the initial water saturation rate, S_{wi} = 0.25; the residual oil saturation, S_{or} = 0.2; the porosity, φ = 0.25; and the oil layer permeability, K = 1.0 mD, obtained Figure 3, which shows the variation law of rock water saturation rate, S_w (dimensionless), with time and dimensionless distance from the borehole axis (r/r_w). Note that, for the convenience of calculations and expressions, the dimensionless distance is used to represent the distance between the calculated formation rock position and the borehole axis, which is represented by r/r_w.

Table 1. Basic calculation data of the model.

Parameter	H/m	p_e/g·cm^{-3}	φ	K/mD	S_{wi}	S_{or}	$\frac{\mu_o}{\mu_w}$	p_b/g·cm^{-3}	r_w/m
value	3100	1.2	0.25	1.0	0.20	0.25	5	1.2	0.12

Note: p_e is formation original pore pressure coefficient; p_b is column pressure coefficient of drilling fluid; r_w is borehole radius.

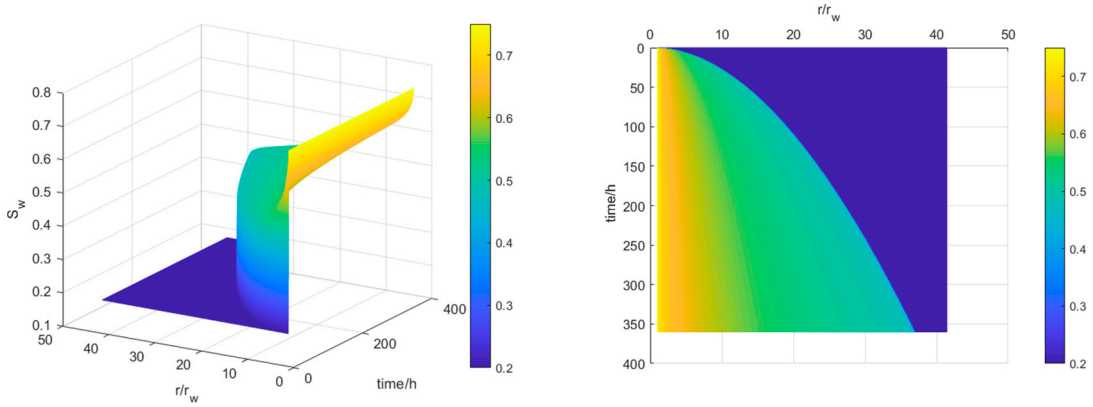

Figure 3. Variation of rock water saturation rate with dimensionless distance and time (3D and 2D).

In Figure 3, the water saturation rate at the wellbore is the highest, and with the extension to the formation, the water saturation rate gradually decreases to the original water saturation rate of the formation. As time passes, the fluctuation radius (dimensionless distance corresponding to the change in the formation water saturation rate) gradually

increases. After 350 h, the fluctuation radius increases to r/r_w = 38. As the water saturation rate changes, and according to Equations (21) and (22), the Young's modulus and Poisson's ratio of the rock will change, and this, in turn, affects the rock's tensile strength (Equation (5)), fracture toughness (Equations (3) and (4)), and fracture pressure (Equations (9) and (10)).

3.3. Variation of Rock Parameters and Fracability after Hydration

According to the calculation results of the water saturation rate, combined with the fracability model, the variation law of each parameter in the FI was calculated. First, the variation laws of YM and μ with dimensionless radial distance at different times were calculated. The results are shown in Figures 4 and 5, respectively.

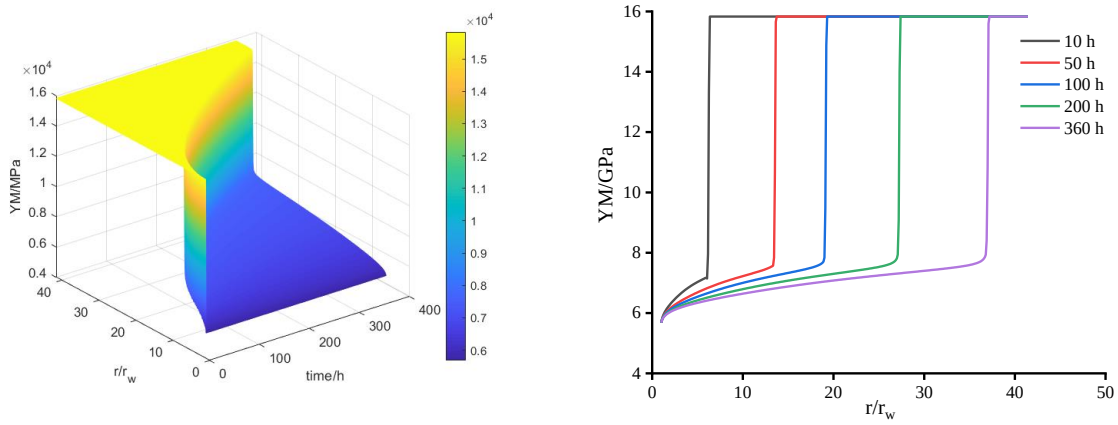

Figure 4. Variation of Young's modulus with dimensionless distance and time.

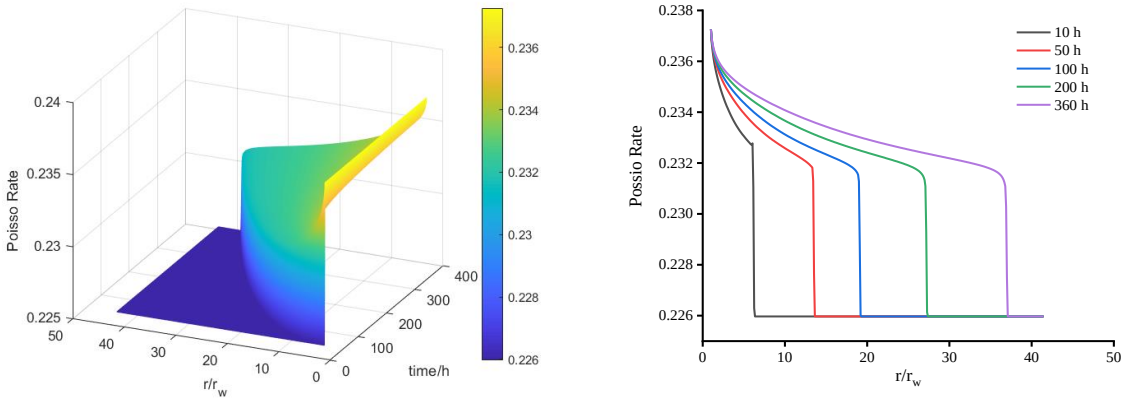

Figure 5. Variation of Poisson's ratio with dimensionless distance and time.

According to the data in Figure 4, the Young's modulus also changed with the change of water saturation rate. Near the wellbore with the highest water saturation rate, the Young's modulus demonstrated the lowest value. As the radial distance increases, the Young's modulus gradually increases and approaches the original value at the edge of the fluctuation radius. By comparing the maximum and the minimum values of the Young's modulus, we found that the change in water saturation rate greatly affects the Young's modulus of rock, from 15.83 GPa to 5.68 GPa, with a decrease of 64.6%.

As shown in Figure 5, with the increase in the water saturation rate, the Poisson's ratio of the rock gradually increases. The original Poisson's ratio of the rock is 0.226, and after hydration, it demonstrates a maximum value of 0.347 near the wellbore, an increase of 53.5%.

According to the calculation model of fracture toughness (Formulas (3) and (4)), the calculation of fracture toughness is closely related to the tensile strength and elastic modulus of the rock. In this paper, the change law of rock fracture toughness is calculated and analyzed. The results are shown in Figure 6.

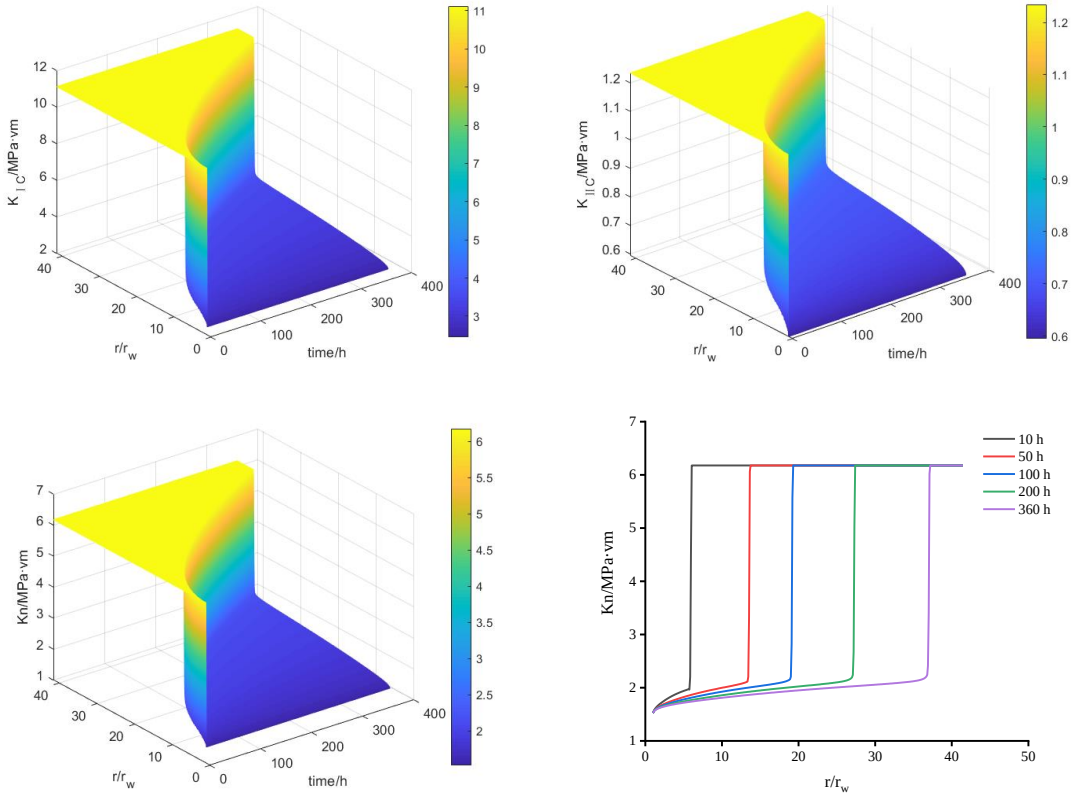

Figure 6. Variation of fracture toughness with dimensionless distance and time ((**left**) type I fracture toughness and (**right**) type II fracture toughness).

Owing to the change in water saturation rate, fracture toughness also exhibits a similar variation law to water saturation rate and Young's modulus. In the near wellbore zone, the rock has a high water saturation rate and low fracture toughness. With the extension from the periphery of the well to the formation, the water saturation rate gradually decreased to the original water saturation rate of the formation, while the fracture toughness also gradually returned to the unhydrated state of the rock.

Based on the above parameters and according to the fracability model, the calculation and analysis of the FI were carried out. The results are shown in Figure 7.

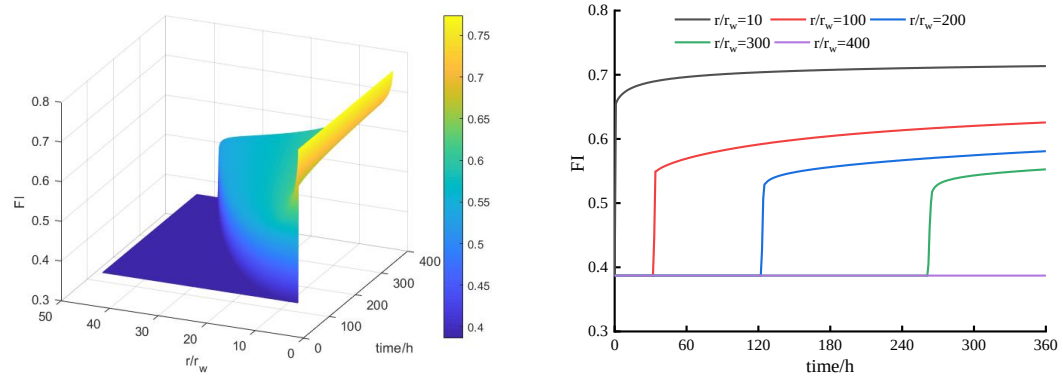

Figure 7. Variation of fracability index with dimensionless distance and time.

Figure 7 shows that the change in water saturation rate changes rock fracability. As the drilling fluid invades the rock, the hydration becomes gradually obvious. The initial FI of the rock at $r/r_w = 10$ is 0.39. After hydration occurs, the FI rises rapidly to 0.71. This shows that hydration has a significant effect on the FI. The rock strength after hydration is reduced and is more prone to fracture. From Figure 3, we observe that, as the dimensionless distance increases, the water saturation rate of the rock gradually decreases, and the FI of the formation rock gradually decreases to the initial value.

4. Case Study

The shale formation in the Da'anzhai Section in Central Sichuan has favorable conditions for lacustrine shale oil and gas accumulation; its high-quality shale is mainly developed in the second sub-member, with favorable conditions such as high organic carbon content, good physical properties, stable distribution, and good oil and gas properties. For example, NC2H is the first shale oil horizontal well in the Sichuan Basin. The depth of the Da'anzhai Section ranges from 2598 to 2703 m.

The method of calculating rock-mechanics parameters from well-logging data has been applied maturely in petroleum engineering. The calculation methods are as shown in Formula (23) [17] (Yuan 2013):

$$\begin{cases} V_{\mathrm{cl}} = \left(2^{G_{\mathrm{cur}}{}^{I}\gamma} - 1\right) / \left(2^{G_{\mathrm{cur}}} - 1\right) \\ I_\gamma = (\gamma - \gamma_{\mathrm{min}}) / (\gamma_{\mathrm{max}} - \gamma_{\mathrm{min}}) \\ E_{\mathrm{d}} = \rho v_{\mathrm{s}}^2 \left(3v_{\mathrm{p}}^2 - 4v_{\mathrm{s}}^2\right) / \left(v_{\mathrm{p}}^2 - 2v_{\mathrm{s}}^2\right) \\ \mu_{\mathrm{d}} = \left(v_{\mathrm{p}}^2 - 2v_{\mathrm{s}}^2\right) / 2\left(v_{\mathrm{p}}^2 - v_{\mathrm{s}}^2\right) \end{cases} \tag{23}$$

where v_p is the longitudinal wave velocity, m/s; v_s is the shear wave velocity, m/s; γ_{max} and γ_{min} are Gamma values of pure sandstone and pure mudstone, respectively; I_γ is argillaceous content index; ρ is rock density, g/cm^3; and G_{cur} is Hilchie index, which is related to geological age. Generally, 37 is taken for Tertiary system and 2 is taken for old stratum.

The in-situ stress calculation methods are as shown in Formula (24) [40] (Huang 1985):

$$\begin{cases} \sigma_V = \int_0^{TVD} \rho g dz = 0.00981 \left(\rho_0 TVD_0 + \sum_{i=1}^{n} \rho_i \Delta TVD_i\right) \\ \sigma_H = \left(\frac{\mu}{1-\mu} + \omega_1\right)(\sigma_v - \alpha P_p) + \alpha P_p \\ \sigma_h = \left(\frac{\mu}{1-\mu} + \omega_2\right)(\sigma_v - \alpha P_p) + \alpha P_p \end{cases} \tag{24}$$

where ω_1 and ω_2 are the tectonic stress coefficient in the direction of maximum and minimum horizontal stress. In the same block, ω_1 and ω_2 are constant; TVD is the vertical depth at measuring, m.

According to the logging data, the Young's modulus, tensile strength, shale content, Poisson's ratio and the in situ stress coefficient are shown in Figure 8. AC and DTS represent P-wave moveout and S-wave moveout, respectively.

According to the logging data, the Young's modulus of the Da'anzhai section of Well NC2H ranges from 18.23 to 23.70 GPa, the tensile strength ranges from 6.27 to 8.18 MPa, the shale content ranges from 0.39 to 0.65, and the Poisson's ratio varies between 0.18 and 0.24. The maximum horizontal principal stress coefficient (σ_{H}) ranges from 2.51 to 3.32, the minimum horizontal principal stress coefficient (σ_{h}) from 2.20 to 2.41, and the vertical in situ stress coefficient (σ_{v}) is about 2.55. The measured parameters are brought into the fracability evaluation model, and the variation law of the FI of the Da'anzhai Section and the depth, time, and dimensionless distance from the wellbore axis are calculated, as shown in Figure 9.

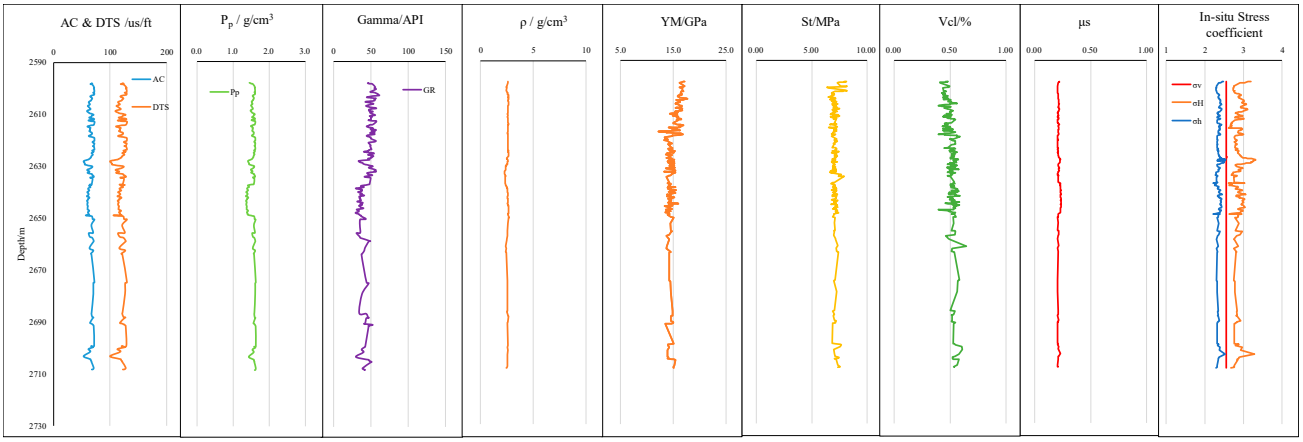

Figure 8. Logging data of the Da'anzhai section (Well NC2H).

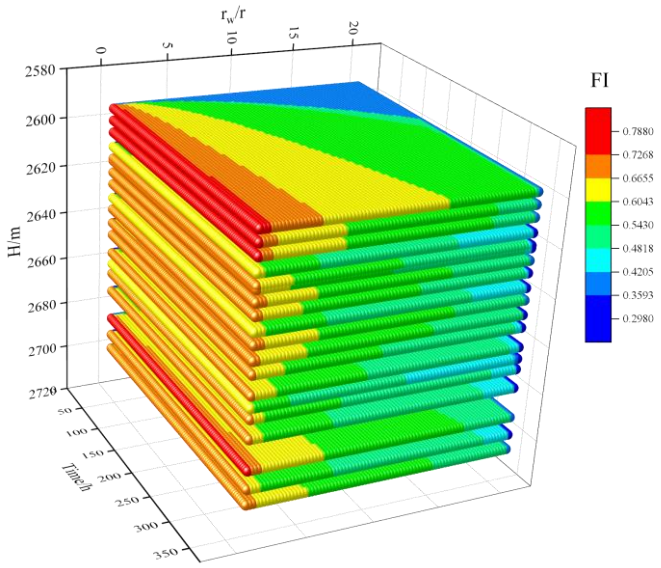

Figure 9. Fracability Index of Da'anzhai Member of Well NC2H.

In Figure 9, the redder the color, the higher the FI and the greater the fracturing feasibility; the bluer the color, the lower the fracturing index and the fracturing feasibility are. Figure 9 shows that, in the Da'anzhai section of Well NC2H, the fracability index at the well wall near 2600 m is 0.78, which is the maximum value in this interval, thus indicating that it is easier to conduct fracturing operations in that region. Simultaneously, at the same depth, the FI near the wellbore is higher because the rock near the wellbore demonstrates a high degree of hydration and is more prone to fracture. The change law of FI with time and dimensionless distance is similar to the change law of water saturation rate in Figure 3. Figure 9 shows that when H = 2600 m, the rock is most likely to fracture. Therefore, according to Formulas (9) and (10), the variations in rock fracture pressure with time and dimensionless distance at a depth of 2600 m were calculated. The results are shown in Figure 10.

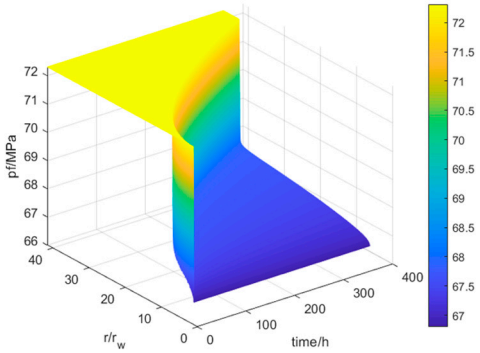

Figure 10. Variation in fracturing pressure with time and dimensionless distance.

According to the data in Figure 10, the fracture pressure near the wellbore is 66.80 MPa, and the original fracture pressure of the formation is 72.31 MPa. The fracturing pressure is the lowest near the borehole wall and gradually increases to the original fracturing pressure of the formation as the distance increases. Combined with the previous variation law of water saturation rate, it shows that after the shale around the well is hydrated, the tensile strength of the rock decreases, and the fracture pressure of the formation decreases. The change in the fracture pressure is similar to the variation law of the water saturation rate of the rock.

5. Conclusions

In this study, the rock mechanical properties of the shale oil reservoirs in the Da'anzhai Section of the Sichuan Basin were discussed, and the fracability index calculation model was established based on three factors: brittleness index, horizontal differential stress, and fracture toughness. A method for evaluating the fracability of shale oil reservoirs, considering hydration, was established. The main conclusions are the following:

1. Through the triaxial mechanical test, we found that the average compressive strength of the immersed rock samples decreased by 37.99%, the average elastic modulus decreased by 53.36%, and the average Poisson's ratio increased by 68.75%. These results show that the mechanical strength and elastic parameters of the shale rock in the Da'anzhai Section are obviously affected by the immersion in the drilling fluid, which further indicates that the change in the water saturation rate of the shale will also change its formation fracability.
2. A fracability evaluation model that comprehensively considers the brittleness index, in situ stress, and fracture toughness was established, and the law of water phase intrusion into shale oil reservoirs was analyzed. The changes in the Young's modulus, Poisson's ratio, fracture toughness, and FI with time and dimensionless distance under hydration were discussed. The results show that the change in the formation FI is closely related to the change in the water saturation rate. The rock at the wellbore is mostly affected by hydration, while the FI is the highest.
3. Taking Well NC2H as an example, the distribution law of the FI of the Da'anzhai section of the well with the well depth, dimensionless distance, and time was calculated and analyzed. The results show that the well is most prone to fracture near H = 2600 m. Second, the variation law of fracture initiation pressure before and after hydration was compared and analyzed, and it was found that the formation fracture initiation pressure decreased after hydration, thus making it easier to conduct fracturing operations.
4. The evaluation method of fracability considering hydration established in this paper cannot only be used to calculate the hydration caused by drilling fluid invading formation during drilling but also the hydration caused by the change in water saturation rate caused by other factors.

Author Contributions: Conceptualization, G.Z. and N.L.; methodology, S.H.; validation, G.Z.; formal analysis, H.W.; investigation, F.L.; resources, D.W.; data curation, G.Z.; writing—original draft preparation, G.Z.; writing—review and editing, S.H.; visualization, H.W.; supervision, N.L.; project administration, N.L.; funding acquisition, H.W. All authors have read and agreed to the published version of the manuscript.

Funding: This research was supported by Evaluation of fracability of continental shale oil reservoir based on mechanochemical coupling (grant Nos. 33550000-21-ZC0613-0307).

Acknowledgments: Thanks to State Key Laboratory of Shale Oil and Gas Enrichment Mechanisms and Effective Development for financial support of this research. Thanks to the support of the State Energy Center for Shale Oil Research and Development. Thanks to the support of Southwest Petroleum University.

Conflicts of Interest: The authors declare no conflict of interest.

References

1. Fathy, D.; Wagreich, M.; Ntaflos, T.; Sami, M. Provenance Characterization of Campanian Lacustrine Organic-Rich Mudstones on the Southern Tethyan Margin, Egypt. *ACS Earth Space Chem.* **2021**, *5*, 197–209. [CrossRef]
2. Du, J.; Hu, S.; Pang, Z.; Lin, S.; Hou, L.; Zhu, R. Types, potential and prospects of continental shale oil in China. *China Pet. Explor.* **2019**, *24*, 560–568.
3. Zou, C.; Yang, Z.; Zhu, R.; Wu, S.; Fu, J.; Lei, D.; Hou, L.; Lin, S.; Pana, S. Geologic significance and optimization technique of sweet spots in unconventional shale systems. *J. Asian Earth Sci.* **2019**, *178*, 3–19. [CrossRef]
4. Zhou, D.; Sun, C.; Liu, Z.; Nie, H. Geological characteristics of continental shale gas reservoirs in Da'anzhai Section, Northeast Sichuan Basin. *China Pet. Explor.* **2020**, *25*, 32–42.
5. Muniz, E.S.; da Fontoura, S.A.B.; Duarte, R.G.; Lomba, R.T.F. Evaluation of the Shale-Drilling Fluid Interaction for Studies of Wellbore Stability. In Proceedings of the Alaska Rocks 2005, The 40th U.S. Symposium on Rock Mechanics (USRMS), Anchorage, AK, USA, 25–29 June 2005.
6. van Oort, E.; Hale, A.H.; Mody, F.K.; Roy, S. Transport in shales and the design of improved water based shale drilling fluids. *SPE Drill. Complet.* **1996**, *11*, 137–146. [CrossRef]
7. Wang, J.; Yan, J.; Su, S. A new method for wellbore stability evaluation of hard and brittle shale. *Pet. Drill. Prod. Technol.* **2006**, *28*, 34–35.
8. Yew, C.H.; Chenevert, M.E.; Wang, C.L. Wellbore Stress Distribution Produced by Moisture Adsorption. *SPE Drill. Eng.* **1990**, *5*, 311–316. [CrossRef]
9. Hale, A.H.; Mody, F.K. The Influence of Chemical Potential on Wellbore Stability. *SPE Drill. Complet.* **1993**, *8*, 207–216. [CrossRef]
10. Zhang, Y.; Sun, J.; Wang, Q. Chemical kinetic analysis of wellbore stability. *Fault Block Oil Gas Fields* **2011**, *18*, 794–798.
11. Deng, Y.; He, S.; Deng, X.; Peng, Y.; He, S.; Tang, M. Study on wellbore instability of bedded shale gas horizontal wells under the action of mechanical-chemical coupling. *Pet. Drill. Technol.* **2020**, *48*, 26–33.
12. Deng, H.; Meng, Y. A review of chemical and mechanical coupling research on mud shale stability. *Pet. Explor. Dev.* **2003**, *30*, 109–111.
13. Rickman, R.; Mullen, M.J.; Petre, J.E.; Grieser, B.; Kundert, D. A practical use of shale petrophysics for stimulation design optimization: All shale plays are not clones of the barnett shale. In Proceedings of the SPE Annual Technical Conference and Exhibition, Denver, CO, USA, 21–24 September 2008.
14. Tang, Y.; Xing, Y.; Li, L.; Zhang, B.H.; Jiang, S.X. Influence factors andevaluation methods of the gas shale fracability. *Earth Sci. Front.* **2012**, *19*, 356–363.
15. Enderlin, M.; Alsleben, H.; Beyer, J.A. Predicting fracability in Shale Reservoirs. In Proceedings of the AAPG Annual Convention and Exhibition, Houston, TX, USA, 10–13 April 2011.
16. Mullen, M.; Enderlin, M. Fracability Index—More Than Just Calculating Rock Properties. In Proceedings of the SPE Annual Technical Conference and Exhibition, San Antonio, TX, USA, 8–10 October 2012.
17. Yuan, J.; Deng, J.; Zhang, D.; Li, D.; Yan, W.; Chen, C.; Cheng, L.; Chen, Z. Evaluation technology for fracability of shale gas reservoirs. *Chin. J. Pet.* **2013**, *34*, 523–527.
18. Zhang, B.; Roegiers, J.C.; Jin, X.; Shah, S.N. Fracability Evaluation in Shale Reservoirs—An Integrated Petrophysics and Geomechanics Approach. In Proceedings of the SPE Hydraulic Fracturing Technology Conference, The Woodlands, TX, USA, 4–6 February 2014. [CrossRef]
19. Guo, T.; Zhang, S.; Ge, H. A new method for evaluating the ability of shale fracturing to form fracture network. *Rock Soil Mech.* **2013**, *34*, 947–954.
20. Li, N.; Zou, Y.S.; Zhang, S.C.; Ma, X.F.; Zhu, X.W.; Li, S.H.; Cao, T. Rock brittleness evaluation based on energy dissipation under triaxial compression. *J. Pet. Sci. Eng.* **2019**, *183*, 106349. [CrossRef]
21. Mullen, M.J.; Enderlin, M.N. Fracability index-more than rock properties. In Proceedings of the SPE Annual Technical Conference and Exhibition, San Antonio, TX, USA, 9 January 2012.

22. Jin, Y.; Chen, M.; Zhang, X. Prediction of rock fracture toughness in deep formations using logging data. *Chin. J. Rock Mech. Eng.* **2001**, *20*, 454–456.
23. Zhao, J.; Xu, W.; Li, Y.; Hu, J.Y.; Li, J.Q. A new method for fracability evaluation of shale-gas reservoirs. *Nat. Gas Geosci.* **2015**, *26*, 1165–1172.
24. Sui, L.; Ju, Y.; Yang, Y.; Hu, J.Y. A quantification method for shale fracability based on analytic hierarchy process. *Energy* **2016**, *115*, 637–645. [CrossRef]
25. Yue, Y. *The Evaluation Method of Tight Reservoir Fracability and the Experimental Investigation of Its Evaluation EFFECT*; Chongqing University: Chongqing, China, 2019.
26. Ma, C.; Dong, C.; Lin, C.; Elsworth, D.; Liu, X. Influencing factors and fracability of lacustrine shale oil reservoirs. *Mar. Pet. Geol.* **2019**, *110*, 463–471. [CrossRef]
27. Jia, Y.; Tang, J.; Lu, Y.; Lu, Z. Laboratory geomechanical and petrophysical characterization of longmaxi shale properties in lower silurian formation, china. *Mar. Pet. Geol.* **2020**, *124*, 104800. [CrossRef]
28. Wu, J.W.; Zhang, S.Z.; Cao, H.C.; Zhao, M.Z.; Sun, P.; Xun, L. Fracability evaluation of shale gas reservoir-a case study in the lower cambrian niutitang formation, northwestern hunan, china—Sciencedirect. *J. Pet. Sci. Eng.* **2018**, *164*, 675–684. [CrossRef]
29. Iyare, U.C.; Blake, O.O.; Ramsook, R. Fracability evaluation of the upper Cretaceous Naparima Hill Formation, Trinidad. *J. Pet. Sci. Eng.* **2022**, *208*, 109599. [CrossRef]
30. Chen, Z.; Li, S.; Chen, Z. Hydraulic Fracture initiation and Extending Tests in Deep Shale Gas Formations and Fracturing Design Optimization. *Pet. Drill. Tech.* **2020**, *48*, 70–76.
31. Lian, G.; Wang, X.; Qin, M. Comprehensive Evaluation Technology of Reservoir Fracability of Mabei Slope in Mahu Area. *J. Southwest Pet. Univ. (Sci. Technol. Ed.)* **2022**, *4*, 1–8.
32. Chen, Z.; Chen, M.; Jin, Y. Experimental study on the relationship between rock fracture toughness and acoustic velocity. *Oil Drill. Prod. Technol.* **1997**, *19*, 56–75.
33. Jin, Y.; Yu, J.; Chen, M. Determination of rock fracture toughness KIIC and its relationship with tensile strength. *Rock Mech. Rock Eng.* **2011**, *44*, 621–627. [CrossRef]
34. Zhao, H.; Chen, M.; Jin, Y.; Ding, Y.; Wang, Y. Rock fracture kinetics of the fracture mesh system in shale gas reservoirs. *Pet. Explor. Dev.* **2012**, *39*, 464–470. [CrossRef]
35. Jin, Y.; Chen, M. *Mechanics of Wellbore Stability*; Science Press: Beijing, China, 2012; pp. 12–20.
36. Buckley, S.E.; Leverette, M.C. Mechanism of fluid displacement in sands. *Trans. AIME* **1942**, *146*, 107–116. [CrossRef]
37. Jiang, Y. *Research on Three-Dimensional Three-Phase Seepage Numerical Simulation of J-Function Average Capillary Force [D]*; Southwest Petroleum University: Chengdu, China, 2014.
38. Naseri, M.; Caglar, S. Numerical Modeling of Counter-Current Spontaneous Imbibition during Underbalanced Drilling. In Proceedings of the North Africa Technical Conference and Exhibition, Cairo, Egypt, 20–22 February 2012. [CrossRef]
39. Huang, R. Coupling study of mechanics and chemistry of shale wellbore stability. *Drill. Complet. Fluids* **1995**, *12*, 15–25.
40. Huang, Z.R.; Zhuang, J.J. A new method for predicting formation fracture pressure. *Oil Drill. Prod. Technol.* **1986**, *8*, 1–14.